Selective heteromeric assembly of cyclic nucleotide-gated channels

Haining Zhong*†, Jun Lai*, and King-Wai Yau*‡§

Departments of *Neuroscience and §Ophthalmology, and ‡Howard Hughes Medical Institute, Johns Hopkins University School of Medicine, Baltimore, MD 21205

Communicated by Lily Y. Jan, University of California School of Medicine, San Francisco, CA, March 5, 2003 (received for review January 30, 2003)

Many ion channels *in vivo* are heteromeric complexes with well defined subunit compositions. For some channels, domains have been identified that determine whether two or more subunit species are compatible in forming a complex. Nonetheless, an unsolved fundamental question is how the native composition of an ion channel is selected during assembly over functional alternatives, such as heteromeric complexes favored over homomers. Cyclic nucleotide-gated channels are tetramers and, in their native forms, are composed of A and B subunits. Although most A subunits can form functional homomeric channels when expressed alone, A/B heteromeric channels are selectively formed in the presence of a B subunit. Here, we show that this selective assembly of heteromeric channels requires a trimer-forming C-terminal leucine zipper (CLZ) domain recently identified in the distal C terminus of A, but not B, subunits. Thus, a CLZ-defective A subunit no longer forms predominantly A/B heteromeric channels with the B subunit. A mechanism for this specificity involving the trimerization of the CLZ domain is proposed.

In many ion channels, assembly domains have been identified (1–6) that enhance the efficiency of channel assembly and/or dictate subunit compatibility in forming a heteromeric channel. However, it is still unclear how a specific stoichiometry of a heteromeric channel is selected out of many combinatorial possibilities from the compatible subunit species. We report here experiments that addressed this question on cyclic nucleotide-gated (CNG) channels. These channels play crucial roles in rod/cone phototransductions and olfactory transduction and, in their native forms, are heterotetramers composed of A and B subunits (7–10). To date, four mammalian A subunits have been cloned and named CNGA1–4 (11), with CNGA1 found in rods, CNGA3 in cones, and CNGA2/CNGA4 in olfactory sensory neurons. Two B subunits are known, named CNGB1 and CNGB3 (CNGB2 does not exist in this nomenclature; ref. 11). When expressed heterologously, several A subunits (CNGA1–3) form functional homomeric channels; B subunits do not, but they form functional heteromeric channels with A subunits. Recently, we have identified a leucine-zipper-homology domain (CLZ) at the distal C terminus of all A subunits but none of the B subunits (Fig. 1*A*; ref. 12). Surprisingly, this domain shows a trimeric, homotypic interaction, which led to the discovery that the native rod CNG channel adopts an unusual stoichiometry of 3A:1B (12). In this work, we report that CLZ is an assembly domain that directs the preferential formation of A/B heteromeric channels. We propose a simple mechanism for this specificity in assembly.

Materials and Methods

Molecular Biology. All of the cDNAs were subcloned into a pRK5 vector and expressed in HEK 293T cells. Chimeras and mutations were made by standard methods. For experiments involving heteromeric CNG channels, we used a cloned version of human (h)CNGB1 (hRCNC2b; ref. 13) instead of CNGB3 because of the difficulty in amplifying mouse CNGB3 (see materials and methods in ref. 14) and because hCNGB1 gives a much higher cAMP/cGMP current ratio (i.e., cAMP has a higher efficacy in activating a heteromeric channel containing CNGB1 than CNGB3), making it easier to identify the formation of A/B heteromers by using this property. Although all of the experiments reported here used CNGA3 and CNGB1, we have also done some experiments with CNGA1 and CNGB1 (the natural combination in retinal rods) and obtained similar results.

Coimmunoprecipitation (co-IP). The experiments were performed at 4°C in IP buffer (1× PBS/5 mM EDTA/5 mM EGTA/1 mM 2-mercaptoethanol) plus indicated components. Two days after calcium phosphate transfection, the cells were lysed in 1% Triton X-100 and spun at 100,000 × *g* for 10 min. The soluble fraction was then incubated with an antibody and protein G Sepharose (Amersham Biosciences) for >2 h. The beads were washed one time with 1% Triton X-100, two times with 1% Triton X-100 plus 500 mM NaCl, and two times with IP buffer. The precipitate was eluted by Laemmli buffer and subjected to Western analysis.

Biotinylation. Two days after transfection, 293T cells were gently washed one time with biotinylation buffer (1× PBS/1 mM $CaCl_2$/0.5 mM $MgCl_2$, made freshly, plus indicated component) and were then incubated with 1 mg/ml sulfosuccinimidyl-6-(biotinamido)hexanoate (Pierce, catalog no. 21335) for 20–30 min at 4°C. The reaction was stopped by two 10-min washes with 100 mM glycine and two washes with biotinylation buffer. The following steps were performed in IP buffer: The biotinylated cells were harvested and solubilized in 1% Triton X-100 at 4°C for 30 min. The lysate was spun at 100,000 × *g* for 10 min and then incubated with prewashed neutravidin beads (200 μl 1:1 slurry; Pierce, catalog no. 53151) for 2 h. The precipitate was then washed as in co-IP experiments.

Electrophysiological Recordings. Zero-Ca^{2+} solution (140 mM NaCl/5 mM KCl/1 mM EDTA/1 mM EGTA/10 mM Hepes/NaOH, pH 7.6) was used on both sides of an excised membrane patch. cGMP or cAMP was added as needed. Macroscopic currents at −60 mV were recorded at room temperature under voltage-clamp from inside-out excised patches at 2–3 days after calcium phosphate transfection. Data were low-pass filtered at 2 kHz (8-pole Bessel) and digitized at 5 kHz. Electrodes of 3–6 MΩ were used. A GFP cDNA was cotransfected to facilitate the identification of transfected cells under a fluorescence microscope. A solenoid-controlled rotary valve system was used to change the bath solution, with a changing time of 1–2 s.

All differences referred to in the bar graph results are statistically significant, based on the Wilcoxon test or the *t′* test.

Results

We first confirmed that the CLZ-mediated interaction takes place in the context of transmembrane proteins. We replaced the C termini of two unrelated transmembrane proteins, hCD4 and

Abbreviations: CNG, cyclic nucleotide-gated; CLZ, C-terminal leucine zipper; co-IP, coimmunoprecipitation.

†To whom correspondence should be addressed at: Johns Hopkins University School of Medicine, 9th Floor, Preclinical Teaching Building, 725 North Wolfe Street, Baltimore, MD 21205. E-mail: hnzhong@mail.jhmi.edu.

NEUROSCIENCE

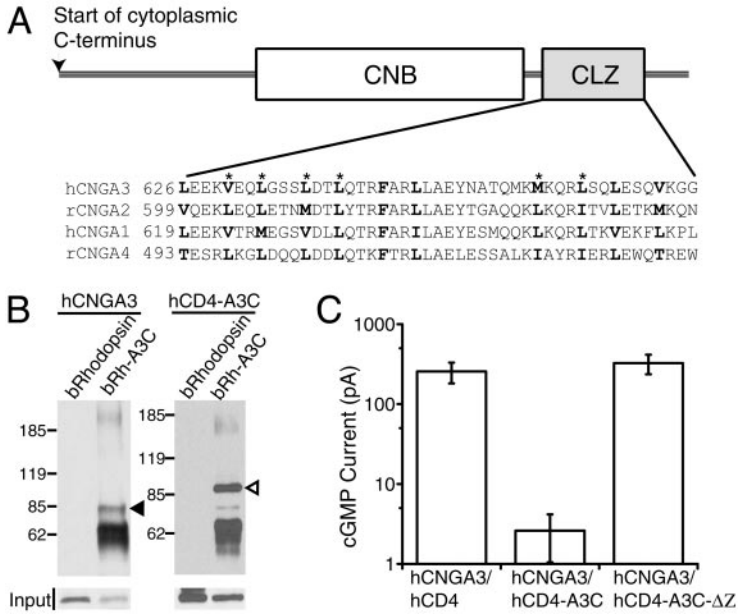

Fig. 1. The CLZ-mediated interaction is important for CNG channel function. (*A*) Cytoplasmic C terminus of CNG channel A subunit, showing the cyclic nucleotide-binding domain (CNB) as an open box and the CLZ domain as a shaded box (adapted from ref. 12). Sequence alignments of the CLZ domains of mammalian CNG channel A subunits are shown underneath (h, human; r, rat). The conserved hydrophobic residues are in bold type. Asterisks label those hydrophobic residues found to be essential for the CLZ-mediated homotypic interaction of hCNGA3 in a coimmunoprecipitation (co-IP) assay (12). (*B*) Co-IP of transmembrane proteins containing the C terminus of hCNGA3. The C termini of bovine rhodopsin (N315-End) and human CD4 (C422-End) were replaced by A3-C (cytoplasmic C terminus of hCNGA3; N398-End) to make A3-C a part of the two transmembrane proteins, bRh-A3C and hCD4-A3C. The hCNGA3 and hCD4-A3C (filled and open arrowhead, respectively) were coimmunoprecipitated with bRh-A3C by an antibody (monoclonal, B6-30) against the N terminus of rhodopsin, but not when wild-type rhodopsin was used instead of bRh-A3C. The hCNGA3 and the chimeras were detected by an antibody (JH 1857) generated in our laboratory against a C-terminal epitope (Y651–K670) of hCNGA3. The lower, robust band in the right lane of both gels represents immunoprecipitated bRh-A3C. Inputs of hCNGA3 and hCD4-A3C before immunoprecipitation are also shown (*Lower*). (*C*) Saturated cGMP-activated currents from excised membrane patches of 293T cells coexpressing hCNGA3 and the indicated transmembrane proteins. The protein level of hCNGA3 was not any lower when hCNGA3 was cotransfected with hCD4-A3C than when it was cotransfected with hCD4, ruling out nonspecific inhibition/competition on the synthesis of hCNGA3 (data not shown). hCD4 is actually a chimeric protein that contains M001–R421 of wild-type hCD4 followed by the C-terminal segment of hCD3ζ (V53-End), a modification irrelevant to our experiments. See *B* for composition of hCD4-A3C. hCD4-A3C-ΔZ is hCD4-A3C with L626–L647 of A3-C deleted. A total of 0.2 μg of cDNA for hCNGA3 and 0.4 μg of cDNA for the other constructs was used for transfection. Means (±SEM) are 255 ± 75 pA (*Left*, 16 patches), 2.6 ± 1.6 pA (*Center*, 14 patches), and 325 ± 89 pA (*Right*, 15 patches).

bovine (b) rhodopsin, with the C terminus of the human cone channel A subunit hCNGA3 (yielding chimeras hCD4-A3C and bRh-A3C), and we found these to interact specifically with each other in a co-IP assay (Fig. 1*B*). Furthermore, in a dominant-negative experiment with excised-patch recording, the cGMP-activated current from expressed hCNGA3 was almost completely suppressed by coexpression with the chimera hCD4-A3C (Fig. 1*C*). This dominant-negative effect was abolished when the CLZ domain in hCD4-A3C was disrupted (hCD4-A3C-ΔZ).

The dominant-negative results described above suggested that CLZ is probably an assembly domain. Indeed, a mutant hCNGA3 lacking the first 22 residues of CLZ (hCNGA3-ΔZ), when expressed in 293T cells, produced a membrane current (excised-patch recordings) ≈16-fold lower than wild type (Fig. 2*A*). Despite the large difference in current amplitudes, the wild-type and mutant channels showed similar cGMP dose–response relations (Fig. 2*B*). They also showed similar *I–V* relations and single-channel behaviors (data not shown), suggesting that the smaller macroscopic current was because of fewer functional channels on the plasma membrane. Finally, when we compared the surface expression of hCNGA3 and hCNGA3-ΔZ by using a biotinylation assay (see *Materials and Methods*), hCNGA3-ΔZ was found at the surface at least as much as hCNGA3 (Fig. 2*C*). Although this result suggests that some hCNGA3-ΔZ protein on the plasma membrane is not in functional channels (perhaps because of the overexpressed protein overrunning the endoplasmic reticulum quality-control system), it nonetheless argues for CLZ being an assembly domain rather than a membrane-targeting signal (15).

Several conserved leucines in the CLZ domain (Fig. 1*A*) are important for assembly. Thus, mutating a single conserved leucine (L633A) decreased the current by half, whereas mutating two leucines (L637S and L640S) decreased the current by ≈50-fold (Fig. 2*D*). Finally, the cGMP-activated current from expressed rCNGA2, an A subunit of the rat olfactory CNG channel, was also reduced by deleting the first 22 residues in its CLZ domain (data not shown), confirming the generality of the results among A subunits.

The CLZ domain turns out to be critical for the selective assembly of heteromeric (i.e., native-like) CNG channels. We measured heteromeric-channel formation by using L-*cis*-diltiazem, a CNG channel blocker with ≈100-fold higher affinity for A/B heteromeric channels than for A homomers (13). In control experiments, the diltiazem dose–response relation for hCNGA3 coexpressed with hCNGB1 (see Fig. 3 legend) fit essentially a single Hill equation with a $K_{1/2}$ ≈100-fold lower than that for hCNGA3 expressed alone (Fig. 3*A*, compare curves 1 and 3), indicating that hCNGA3 formed predominantly (close to 100% in terms of current; see also ref. 16) heteromeric channels in the presence of hCNGB1 (Fig. 3*A Right*; see legend for details). The results with the CLZ-defective hCNGA3 mutant, L633A (same mutant as in Fig. 2*D*), were quite different. Although the diltiazem dose–response relation for L633A alone was very similar to that for

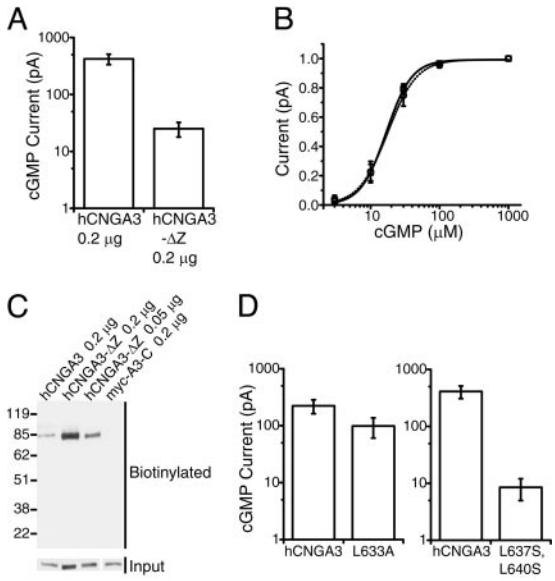

Fig. 2. Involvement of CLZ domain in assembly of functional CNG A homomeric channels. (*A*) Saturated cGMP-activated current amplitudes from excised patches containing expressed hCNGA3 or hCNGA3-ΔZ (hCNGA3 with L626–L647 deleted). Means (±SEM) are 421 ± 87 pA (*Left*, 14 patches) and 25 ± 7 pA (*Right*, 17 patches). (*B*) cGMP dose–response relations of expressed hCNGA3 (squares and solid line, eight patches) and hCNGA3-ΔZ (circles and dashed line, nine patches). Data were normalized to currents activated by 1 mM cGMP and fitted by the Hill equation with $K_{1/2}$ = 16.9 μM, n = 2.3 (hCNGA3), and $K_{1/2}$ = 17.8 μM, n = 2.1 (hCNGA3-ΔZ). The error bars are SDs. (*C*) Levels of biotinylated hCNGA3, hCNGA3-ΔZ, and presumably soluble myc-A3-C (myc-tagged cytoplasmic C terminus of hCNGA3, negative control) are compared. The surface proteins of transfected 293T cells were labeled with a membrane-impermeant biotinylation reagent. The biotinylated proteins were purified with avidin beads and subjected to immunoblot analysis with the antibody (JH 1857) against the C terminus of hCNGA3. (*D*) Saturated cGMP-activated current amplitudes from hCNGA3 vs. two mutant channels carrying point mutations in their CLZ domains (L633A and L637S, L640S). Means (±SEM) are 223 ± 61 pA (*Left*, 13 patches, hCNGA3), 98 ± 38 pA (*Left*, 14 patches, L633A), 410 ± 102 pA (*Right*, 15 patches, hCNGA3), and 8.5 ± 3.5 pA (*Right*, 15 patches, L637S, L640S).

wild-type homomeric channels (Fig. 3*A*, curve 4), the relation for L633A/hCNGB1 showed two components, with characteristics of homomeric and heteromeric channels, respectively (Fig. 3*A*, curve 2). By fitting with a linear combination of two Hill equations, the average fraction of heteromeric current was estimated to be only 35% (Fig. 3*A Right*). Thus, there appeared to be a strong preference for forming heteromeric channels when wild-type hCNGA3 was coexpressed with hCNGB1, and this preference depended on an intact CLZ domain. Besides the diltiazem block, the L633A mutant with hCNGB1 also gave a much smaller current (≈20-fold lower than L633A alone), unlike wild type (Fig. 3*B*), suggesting that far fewer functional channels were formed.

The conclusion that L633A failed to selectively form heteromeric channels in the presence of hCNGB1 was confirmed by a separate experiment. Unlike cGMP, cAMP is known to activate the A/B heteromeric channel with a much higher efficacy than it does the A homomeric channel (17). Therefore, the saturated cAMP-activated/saturated cGMP-activated current ratio can be used as an indicator of heteromeric-channel formation. As expected, wild-type hCNGA3 showed a substantial increase in the cAMP/cGMP current ratio in the presence of hCNGB1 (Fig. 4*A*; see also ref. 18). This ratio, comparable to that measured in native photoreceptors, was practically unchanged over a 20-fold variation in the amount of transfected hCNGB1 cDNA. The CLZ-defective hCNGA3 mutant (L633A), on the other hand, produced currents with a cAMP/cGMP current ratio intermediate between those for A homomeric and wild-type A/B heteromeric channels when coexpressed with hCNGB1 (Fig. 4*B*), again suggesting a mixed presence of homomeric and heteromeric channels. A qualitatively similar effect was observed with another hCNGA3 mutant (L662S/L665S; data not shown). Finally, the same conclusions were derived from analyzing channel open probabilities induced by cAMP in excised, single-channel patches (data not shown). Thus, we conclude that the CLZ domain is important for the selective formation of heteromeric CNG channels.

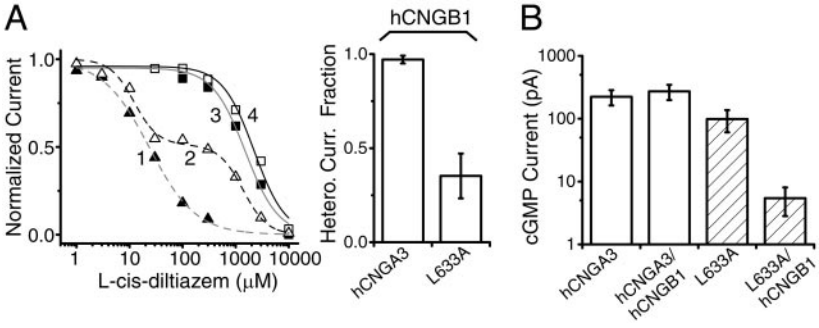

Fig. 3. The CLZ domain is critical for preferential formation of A/B heteromers. (*A*) L-*cis*-Diltiazem block of hCNGA3 and its point mutant L633A, either expressed alone or coexpressed with hCNGB1. (*Left*) The representative dose–response relations from one experiment: curves 1–4 are those of hCNGA3/hCNGB1, L663A/hCNGB1, hCNGA3, and L663A, respectively. (*Right*) The averaged fraction of total current from heteromeric channels for hCNGA3 and L633A coexpressed, respectively, with hCNGB1 (see below for fitting method and values). The data for hCNGA3 and L633A expressed alone were fitted with the ORIGIN program (Microcal Software, Northampton, MA) by the Hill equation, $I = I_{max}[K_{1/2}{}^n/(K_{1/2}{}^n + C^n)]$. (*Left*) The fitting parameters were $K_{1/2}$ = 1.52 mM, n = 1.40 (hCNGA3), and $K_{1/2}$ = 2.22 mM, n = 1.46 (L633A). Means (±SEM) from five patches were $K_{1/2}$ = 2.28 ± 0.28 mM, n = 1.34 ± 0.09 (hCNGA3) and $K_{1/2}$ = 1.69 ± 0.37 mM, n = 1.46 ± 0.22 (L633A). The data in the presence of hCNGB1 were fitted with a linear combination of two Hill equations, $I = f[K_{1/2}{}^n/(K_{1/2}{}^n + C^n)] + (1 - f)[K'_{1/2}{}^{n'}/(K'_{1/2}{}^{n'} + C^{n'})]$, with the five parameters optimized to provide the best fit. (*Left*) The optimized parameters are f = 1, $K_{1/2}$ = 23.6 μM, n = 0.99 for hCNGA3/hCNGB1, and f = 0.48, $K_{1/2}$ = 12.2 μM, n = 1.94, $K'_{1/2}$ = 1.38 mM, n' = 1.91 for L633A/hCNGB1. The mean values (±SEM) for heteromers (four patches each) are f = 0.97 ± 0.02, $K_{1/2}$ = 27.0 ± 2.3 μM, n = 0.94 ± 0.03, $K'_{1/2}$ = 4.65 ± 0.39 mM, n' = 5.49 ± 2.49 for hCNGA3/hCNGB1, and f = 0.35 ± 0.12, $K_{1/2}$ = 22.6 ± 6.5 μM, n = 1.42 ± 0.33, $K'_{1/2}$ = 2.00 ± 0.36 mM, n' = 1.68 ± 0.18 for L633A/hCNGB1. Note that $K'_{1/2}$ and n' values for hCNGA3/hCNGB1 are rough because the homomer fraction is too small. (*B*) Macroscopic (saturated) cGMP-activated currents for hCNGA3 and its point mutant L633A, either expressed alone or coexpressed with hCNGB1. A total of 0.1 μg of each cDNA was transfected. Mean currents (±SEM) are 223 ± 61 pA (13 patches, hCNGA3), 272 ± 74 pA (13 patches, hCNGA3/hCNGB1), 99 ± 38 pA (14 patches, L633A), and 5.4 ± 2.6 pA (13 patches, L633A/hCNGB1). Although more channels might be expected from the same amount of transfected hCNGA3 cDNA in the presence of hCNGB1 than in its absence, the current was not significantly larger in the former case, presumably because of the flickery openings of the heteromeric channels and therefore smaller effective single-channel currents (13).

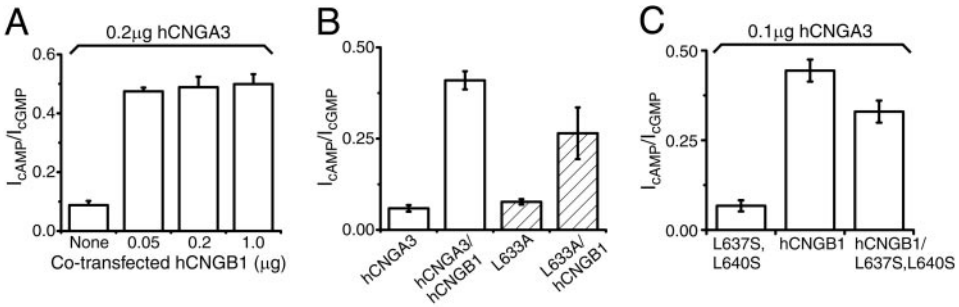

Fig. 4. Saturated cAMP-activated/saturated cGMP-activated current ratios. (*A*) hCNGA3 (0.2 μg per dish) was coexpressed with indicated amounts of hCNGB1 (six patches in each condition). Means (±SEM) are 0.088 ± 0.014 (no hCNGB1), 0.475 ± 0.012 (0.05 μg of hCNGB1), 0.489 ± 0.036 (0.2 μg of hCNGB1), and 0.499 ± 0.034 (1 μg of hCNGB1). The cAMP/cGMP current ratio did decrease when the amount of transfected hCNGB1 was <0.05 μg per dish (data not shown). (*B*) hCNGA3 and its point mutant L633A, either expressed alone or coexpressed with hCNGB1. A total of 0.1 μg of each cDNA was transfected. Average ratios are 0.059 ± 0.009 (seven patches, hCNGA3), 0.409 ± 0.025 (seven patches, hCNGA3/hCNGB1), 0.077 ± 0.007 (eight patches, L633A), and 0.265 ± 0.071 (seven patches, L633A/hCNGB1). (*C*) hCNGA3 was coexpressed with hCNGB1 and/or the CLZ-defective hCNGA3 mutant (L637S, L640S). Means (±SEM, five patches each) are 0.067 ± 0.015 (hCNGA3/L637S, L640S), 0.444 ± 0.031 (hCNGA3/hCNGB1), and 0.330 ± 0.031 (hCNGA3/hCNGB1/L637S, L640S).

Discussion

One of our findings, namely that a CNG channel A subunit lacking the CLZ domain does not form functional homomeric channels efficiently, is different from the recently reported result (19, 20) based on expression in *Xenopus* oocytes that a bCNGA1 mutant lacking the distal C terminus (the sequence immediately after the cyclic nucleotide-binding site) readily formed homomeric channels. The currents from wild-type or mutant CNGA1 in the previous work are ≈10-fold higher than the wild-type current we obtained (and apparently even higher in current density than on native rods; refs. 21 and 22), suggesting a much higher protein-expression level under their conditions. Possibly, the high concentration of mutant monomer on the endoplasmic reticulum membrane of *Xenopus* oocytes was able to compensate for the loss of the appropriate assembly domain; an analogous situation applies to the T1-domain-deleted Kv potassium channel, which is also functionally expressible but requires much higher mRNA concentrations and longer time (23). When we transfected a 10-fold higher amount of hCNGA3 cDNA into HEK 293T cells to boost channel expression, however, the cells became very sick (unpublished observation), suggesting that this mammalian cell line could not support an extremely high level of expression of this channel. Despite the discrepancy with respect to homomeric-channel expression, our more important observation on heteromeric-channel formation is consistent with that of Bennett *et al.* (20), who, in the context of an entirely different question, reported that channels formed in *Xenopus* oocytes by the C-terminal-truncated A subunit and a wild-type B subunit have a sensitivity to L-*cis*-diltiazem intermediate between the sensitivities of homomeric and heteromeric channels.

Two features of the CLZ domain, likely related, are particularly provocative: (*i*) in contrast to the assembly domains previously characterized in other channels (1–6), this domain is not common to all subunits that assemble in the final channel complex, and (*ii*) the domain favors the formation of heteromers over that of homomers. How can the CLZ domain help the A subunit assemble with the B subunit, which does not even have this domain? Because the CLZ domain forms a trimer (12), and the native heteromeric CNG channel adopts a 3A:1B stoichiometry (12, 24, 25), the following model can be formulated for the preferential assembly of heteromeric CNG channels (Fig. 5*A*). In this model, the A monomers are quickly depleted after synthesis by the formation of CLZ-mediated trimeric intermediates. In the absence of the B subunit, residual and newly synthesized A monomers presumably can complete the tetrameric complex, because functional homomeric channels were still observed. However, in the presence of the B subunit, the abundant B monomers dominate the last step and assemble with the trimeric A intermediates to form 3A:1B heteromeric channels. With a defective CLZ domain, the mutant A subunit loses its tendency to form the trimeric intermediate, leaving monomers in abundance (Fig. 5*B*). Thus, the mutant A monomers can compete against the B subunit in the last step of assembly to produce a mixture of A homomeric and A/B heteromeric channels. The fact that such a CLZ-defective A subunit produces only a small current when coexpressed with the B subunit (Fig. 3*B*) suggests that any complex containing more than one B subunit may be nonfunctional. The above model predicts that a CLZ-defective A subunit coexpressed with both wild-type A and B subunits should produce a mixture of A homomeric and A/B heteromeric channels. Indeed, a lower cAMP/cGMP current ratio was observed in such an experiment (Fig. 4*C*) with a CLZ-defective mutant (L637S, L640S; Fig. 2*D*), indicative of mixed

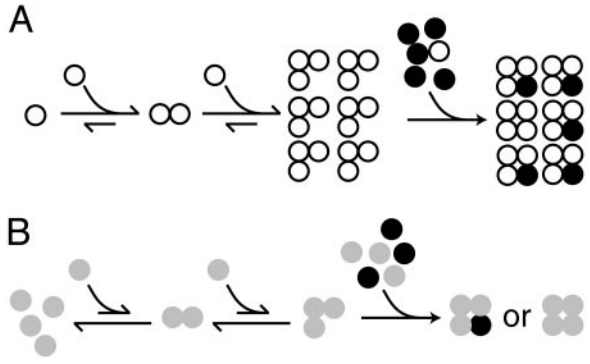

Fig. 5. A model for the assembly of heteromeric CNG channels. (*A*) The monomers of wild-type A subunits (white circles) are quickly depleted to form trimeric assembly intermediates after they are synthesized. In the last step of the channel assembly, the B subunit (black circles) is dominant because its monomer concentration is much higher than the A monomers, and the 3A:1B heteromeric channels are preferentially produced. (*B*) The CLZ-disrupted mutant A subunits (gray circles) have a much smaller tendency to form the trimeric intermediate, and the monomer concentration remains high. The mutant A monomers can then compete with the B monomers to form a mixture of A homomeric and A/B heteromeric channels. Our data also suggest that a complex with more than one B subunit may be nonfunctional (see text). In any case, the likelihood of more than one B subunit in a wild-type complex is low because the wild-type A subunit already forms mostly trimers.

homomer/heteromer formation. The above model and experiment do not exclude an additional factor such as a higher affinity of the B monomer than the A monomer for the A trimeric intermediate during assembly.

Until now, the determinants for the selective heteromeric assembly of tetrameric channels have been unclear. We have described here a possible mechanism of how this may happen by involving a trimeric CLZ domain, which dictates the formation of a specific 3A:1B stoichiometry of the heterotetrameric CNG channel. It will be interesting to see whether related mechanisms are used for assembling other tetrameric channel complexes, perhaps involving yet unidentified assembly domains.

We thank Dr. M. Biel for the mCNGB3 cDNA, Dr. J. Nathans for the B6-30 monoclonal antibody, and Drs. R. H. Huganir, M. Li, J. Nathans, F. Rupp, and D. T. Yue for helpful suggestions on the experiments. Drs. M. Li, D. T. Yue, and J. N. Bradley provided invaluable comments on the manuscript. This work was supported in part by a grant from the U.S. National Eye Institute.

1. Li, M., Jan, Y. N. & Jan, L. Y. (1992) *Science* **257,** 1225–1230.
2. Shen, N. V., Chen, X., Boyer, M. M. & Pfaffinger, P. J. (1993) *Neuron* **11,** 67–76.
3. Tinker, A., Jan, Y. N. & Jan, L. Y. (1996) *Cell* **87,** 857–868.
4. Daram, P., Urbach, S., Gaymard, F., Sentenac, H. & Cherel, I. (1997) *EMBO J.* **16,** 3455–3463.
5. Ludwig, J., Owen, D. & Pongs, O. (1997) *EMBO J.* **16,** 6337–6345.
6. Quirk, J. C. & Reinhart, P. H. (2001) *Neuron* **32,** 13–23.
7. Finn, J. T., Grunwald, M. E. & Yau, K. W. (1996) *Annu. Rev. Physiol.* **58,** 395–426.
8. Zagotta, W. N. & Siegelbaum, S. A. (1996) *Annu. Rev. Neurosci.* **19,** 235–263.
9. Biel, M., Zong, X., Ludwig, A., Sautter, A. & Hofmann, F. (1999) *Rev. Physiol. Biochem. Pharmacol.* **135,** 151–171.
10. Kaupp, U. B. & Seifert, R. (2002) *Physiol. Rev.* **82,** 769–824.
11. Bradley, J., Frings, S., Yau, K. W. & Reed, R. (2001) *Science* **294,** 2095–2096.
12. Zhong, H., Molday, L. L., Molday, R. S. & Yau, K. W. (2002) *Nature* **420,** 193–198.
13. Chen, T. Y., Peng, Y. W., Dhallan, R. S., Ahamed, B., Reed, R. R. & Yau, K. W. (1993) *Nature* **362,** 764–767.
14. Gerstner, A., Zong, X., Hofmann, F. & Biel, M. (2000) *J. Neurosci.* **20,** 1324–1332.
15. Ma, D., Zerangue, N., Lin, Y. F., Collins, A., Yu, M., Jan, Y. N. & Jan, L. Y. (2001) *Science* **291,** 316–319.
16. He, Y., Ruiz, M. & Karpen, J. W. (2000) *Proc. Natl. Acad. Sci. USA* **97,** 895–900.
17. Gordon, S. E., Oakley, J. C., Varnum, M. D. & Zagotta, W. N. (1996) *Biochemistry* **35,** 3994–4001.
18. Shammat, I. M. & Gordon, S. E. (1999) *Neuron* **23,** 809–819.
19. Trudeau, M. C. & Zagotta, W. N. (2002) *Neuron* **34,** 197–207.
20. Bennett, N., Ildefonse, M., Pages, F. & Ragno, M. (2002) *Biophys. J.* **83,** 920–931.
21. Haynes, L. W., Kay, A. R. & Yau, K. W. (1986) *Nature* **321,** 66–70.
22. Karpen, J. W., Loney, D. A. & Baylor, D. A. (1992) *J. Physiol. (London)* **448,** 257–274.
23. Zerangue, N., Jan, Y. N. & Jan, L. Y. (2000) *Proc. Natl. Acad. Sci. USA* **97,** 3591–3595.
24. Zheng, J., Trudeau, M. C. & Zagotta, W. N. (2002) *Neuron* **36,** 891–896.
25. Weitz, D., Ficek, N., Kremmer, E., Bauer, P. J. & Kaupp, U. B. (2002) *Neuron* **36,** 881–889.